Military Technical College
Kobry El-Kobbah,
Cairo, Egypt

6th International Conference
on Electrical Engineering
ICEENG 2008

Characterization of lighting electromagnetic fields and their modeling

By

V.A. Rakov*

Abstract:

Characteristics of measured electric and magnetic fields generated by leaders and return strokes in lightning cloud-to-ground discharges are reviewed. The very close (within tens to hundreds of meters) lightning electromagnetic environment is discussed. Typical field waveforms at distances ranging from 10 m to 200 km are shown. Modeling of lightning return strokes as sources of electromagnetic fields is reviewed. Four classes of models, defined on the basis of the type of governing equations, are considered. These four classes are: 1) gas-dynamic models, 2) electromagnetic models, 3) distributed-circuit models, and 4) engineering models. Model-predicted fields are compared with measurements.

Keywords:

Lightning, electromagnetic fields, measurements, modeling

* Department of Engineering and Computer Engineering, University of Florida, Gainesville, Florida, USA

1. Introduction:

Knowledge of the characteristics of electric and magnetic fields produced by lightning discharges is needed for studying the effects of the potentially deleterious coupling of lightning fields to various circuits and systems. Sensitive electronic circuits are particularly vulnerable to such effects. The computation of lightning electric and magnetic fields requires the use of a model that specifies current as a function of time at all points along the radiating lightning channel. The computed fields can be used as an input to electromagnetic coupling models, the latter, in turn, being used for the calculation of lightning induced voltages and currents in various circuits and systems. In this tutorial lecture, lightning electric and magnetic fields measured at distances ranging from 10 m to 200 km will be characterized and discussed. Then, various lightning models will be reviewed, and model-predicted fields will be compared to measurements.

2. Measured Electric and Magnetic Fields:

In this section, we will discuss measurements of vertical and horizontal electric and horizontal magnetic fields produced by negative return strokes on microsecond and sub-microsecond time scales. A review of measured fields due to positive return strokes and due to lightning processes other than return strokes in both cloud-to-ground and cloud flashes is found in Rakov (1999) [1].

2.1 Distance range from 1 to 200 km

Typical vertical electric and horizontal magnetic field waveforms at distances ranging from 1 to 200 km for both first and subsequent strokes were published by Lin et al. (1979) [2]. These waveforms, which are drawings based on the many measurements acquired in Florida, are reproduced in Fig. 1.

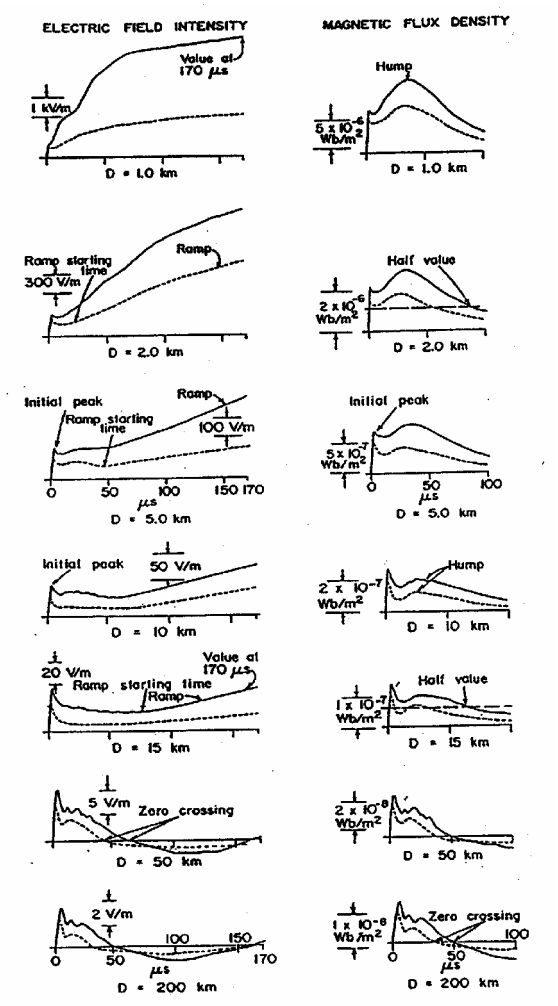

Fig. 1. Typical vertical electric field intensity (left column) and horizontal magnetic flux density (right column) waveforms for first (solid line) and subsequent (dashed line) return strokes at distances of 1, 2, 5, 10, 15, 50, and 200 km. Adapted from Lin et al. (1979) [2].

The electric fields of strokes within a few kilometers, shown in Fig. 1, are, after the first few tens of microseconds, dominated by the electrostatic component of the total electric field, the only field component which is nonzero after the stroke current has ceased to flow. The close magnetic fields at similar times are dominated by the magnetostatic component of the total magnetic field, the component that produces the magnetic field humps seen in Fig. 1. Distant electric and magnetic fields have essentially identical waveshapes and are usually bipolar, as illustrated in Fig. 1. The data of Lin et al. (1979) [2] suggest that at a distance of 50 km and beyond both electric and magnetic field waveshapes are composed primarily of the radiation component of the respective total fields. The initial field peak evident in the waveforms of Fig. 1 is the dominant feature of the electric and magnetic field waveforms beyond abut 10 km, is a significant feature of waveforms from strokes

between a few and about 10 km, and can be identified, with some effort, in waveforms for strokes as close as a kilometer. The initial field peak is due to the radiation component of the total field and, hence, decreases inversely with distance in the absence of significant propagation effects (Lin et al. 1979, 1980 [2,3]). Thus the initial field peaks produced by different return strokes at known distances can be range normalized for comparison, for example, to 100 km by multiplying the measured field peaks by $r/10^5$ where r is the stroke distance in meters. Statistics on the normalized initial electric field peak, derived from selected studies, are presented in Table 1. The mean of the electric field initial peak value, normalized to 100 km, is generally found to be in the range 6-8 V m^{-1} for first strokes and 3-6 V m^{-1} for subsequent strokes. Higher observed mean values are likely to be an indication of the fact that small strokes were missed because the equipment trigger threshold was set too high (e.g., Krider and Guo 1983 [4]). Since the initial electric field peak appears to obey a log-normal distribution, the geometric mean value (equal to the median value for a log-normal distribution) may be a better characteristic of the statistical distribution of this parameter than the mean (arithmetic mean) value. Note that the geometric mean value for a log-normal distribution is lower than the corresponding mean value and higher than the modal (most probable) value. About one third of multiple-stroke flashes have at least one subsequent stroke that is larger than the first stroke in the flash (Thottappilllil et al. 1992; Rakov et al. 1994 [5,6]). Details of the shape of the return-stroke field rise to peak and the fine structure after the initial peak are shown in Fig. 2, and some measured characteristics are summarized in Table 1. Note that also shown in Fig. 2 are stepped-leader pulses occurring prior to the return stroke field. As illustrated in Fig. 2, first return stroke fields have a "slow front" (below the dotted line in Fig. 2 and labeled F) that rises in a few microseconds to an appreciable fraction of the field peak. Master et al. (1984) [7] found a mean slow front duration of 2.9 μs with about 30 percent of the initial field peak being due to the slow front. Cooray and Lundquist (1982) [8] report corresponding values of 5 μs and 41 percent. Weidman and Krider (1978) [9] find the mean slow front duration of about 4.0 μs with 40-50 percent of the initial field peak attributable to the slow front. The slow front is followed by a "fast transition" to peak field (labeled R in Fig. 2) with a 10-90 percent risetime of about 0.1 μs when the field propagation path is over salt water. Weidman and Krider (1980a, 1984) [10,11] and Weidman (1982) [12] report a mean risetime of 90 ns with a standard deviation of 40 ns for 125 first strokes. As illustrated in Fig. 2 fields from subsequent strokes have fast transitions similar to those of first strokes except that these transitions account for most of the rise to peak, while the slow fronts are of shorter duration than for first strokes, typically 0.5-1 μs and only comprise about 20 percent of the total rise to peak (Weidman and Krider 1978 [9]).

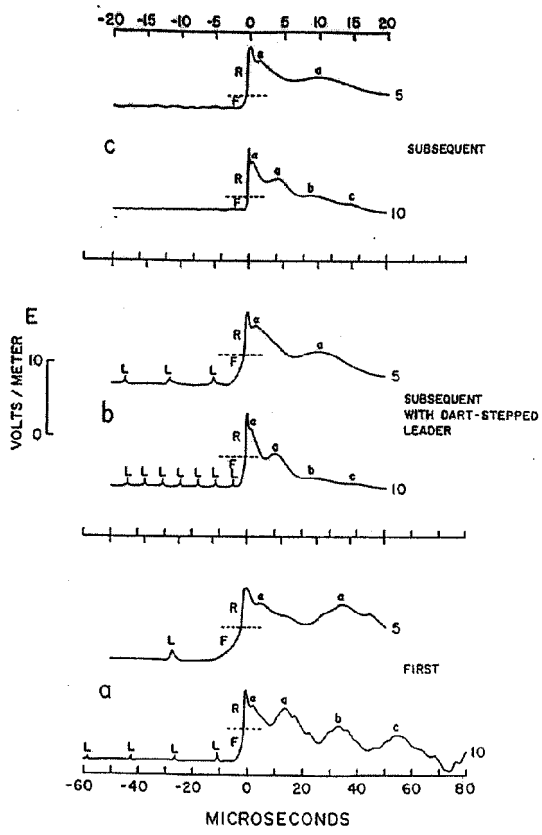

Fig. 2. Electric field waveforms of (a) first return stroke, (b) subsequent return stroke initiated by a dart-stepped leader, and (c) subsequent return stroke initiated by a dart leader. Each waveform is shown on two time scales, 5 μs/div (labeled 5) and 10 μs/div (labeled 10). The waveforms are normalized to a distance of 100 km. L denotes individual leader pulses, F slow front, and R fast transition. See text for details. Also marked are small secondary peak or shoulder α and larger subsidiary peaks a, b, and c. Adapted from Weidman and Krider (1978) [9].

The high frequency content of the return-stroke fields is preferentially degraded in propagating over a finitely conducting earth (Uman et al. 1976 [13]; Lin et al. 1979 [2]; Weidman and Krider 1980a, 1984 [10,11]; Cooray and Lundquist 1983 [14]) so that the fast transition and other rapidly changing fields can only be adequately observed if the propagation path from the lightning to the antenna is over salt water, a relatively good conductor. It is for that reason that the fast transition time observed by Master et al. (1984) [7] for lightning in the 1- to 20-km range over land is an order of magnitude greater than that observed over salt water by Weidman and Krider (1980a, 1984) [10,11] and Weidman (1982) [12] (see Table 1). Lin et al. (1979) [2] report from two-station measurements that normalized field peaks are typically attenuated 10 percent in propagating over 50 km of Florida soil and 20 percent in propagating 200 km. Uman et al. (1976) [13] reported on field risetimes observed both near a given stroke and 200 km from it. For typical strokes, zero-to-peak risetimes (see Table 1) are increased of the order of

Table 1. Parameters of microsecond-scale electric field waveforms produced by negative return strokes.

Parameter	Location	First strokes			Subsequent strokes		
		Sample size	Mean	SD	Sample size	Mean	SD
Initial peak (normalized to 100 km) (V/m)							
Rakov and Uman (1990b)	Florida	76	5.9 (GM)		232*	2.7(GM)	
					38†	4.1(GM)	
Cooray and Lundquist (1982)	Sweden	553	5.3	2.7			
Lin et al. (1979)	KSC	52	6.7	3.8	83	5.0	2.2
	Ocala	29	5.8	2.5	59	4.3	1.5
Zero-crossing time (μs)							
Cooray and Lundquist (1985)	Sweden	102	49	12	94	39	8
	Sri Lanka	91	89	30	143	42	14
Lin et al. (1979)	Florida	46**	54	18	77**	36	17
Zero-to-peak risetime (μs)							
Master et al. (1984)	Florida	105	4.4	1.8	220	2.8	1.5
Cooray and Lundquist (1982)	Sweden	140	7.0	2.0			
Lin et al. (1979)	KSC	51	2.4	1.2	83	1.5	0.8
	Ocala	29	2.7	1.3	59	1.9	0.7
10-90 percent risetime (μs)							
Master et al. (1984)	Florida	105	2.6	1.2	220	1.5	0.9
Slow front duration (μs)							
Master et al. (1984)	Florida	105	2.9	1.3			
Cooray and Lundquist (1982)	Sweden	82	5.0	2.0			
Weidman and Krider (1978)	Florida	62	4.0	1.7	44	0.6	0.2
		90	4.1	1.6	120	0.9	0.5
					34††	2.1	0.9
Slow front, amplitude as percentage of peak							
Master et al. (1984)	Florida	105	28	15			
Cooray and Lundquist (1982)	Sweden	83	41	11			
Weidman and Krider (1978)	Florida	62	50	20	44	20	10
		90	40	20	120	25	10
					34††	40	20
Fast transition, 10-90 percent risetime (ns)							
Master et al. (1984)	Florida	102	970	680	217	610	270
Weidman and Krider (1978)	Florida	38	200	100	80	200	40
		15	200	100	34	150	100
Weidman and Krider (1980a, 1984) Weidman (1982)	Florida	125	90	40			
Peak time derivative (normalized to 100 km) (V m^{-1} s^{-1}) Krider et al. (1998)	Florida	63	63	11			
Time derivative pulse width at half-peak value (ns) Krider et al. (1998)	Florida	61	100	20			

If not specified otherwise, multiple lines for a given source for the same location correspond to different thunderstorms.
GM = geometric mean value, a better characteristic of the distribution of initial field peaks since this distribution is approximately log-normal.
* Strokes following previously formed channel.
† Strokes creating new termination on ground.
**Both electric and magnetic fields.
†† Subsequent strokes initiated by dart-stepped leaders. Other subsequent strokes studied by Weidman and Krider (1978) were initiated by dart leaders.
1 μs in propagating 200 km across Florida soil.

We now briefly discussed measurements of the horizontal component of electric field due to lightning return strokes. Thomson et al. (1988) [15] presented simultaneously measured horizontal and vertical electric fields for 42 return strokes in 27 Florida flashes at distances ranging from 7 to 43 km. The horizontal field waveforms

exhibited relatively narrow initial peaks having a mean width at half-peak level of 0.52 μs. The mean ratio of horizontal field peak to the corresponding vertical field peak was found to be 0.030 and the standard deviation was 0.007. The horizontal electric field appears to be similar in its waveshape to the derivative of the vertical electric field.

2.2 Distance range from 10 to 500 m:

Rubinstein et al. (1995) [16] analyzed vertical electric field waveforms for 31 leader/return-stroke sequences at 500 m and 2 leader/return-stroke sequences at 30 m from the lightning channel. The lightning flashes were triggered using the classical rocket-and-wire technique at the Kennedy Space Center, Florida, in 1986 and 1991, respectively. Rubinstein et al. (1995) [16] found that at tens to hundreds of meters from the lightning channel the combined leader/return-stroke vertical electric field waveforms appear as asymmetric V-shaped pulses, with the trailing (return-stroke) edge of the pulse being sharper than the leading (leader) edge. The bottom of the V is associated with the transition from the leader to the return stroke. Since 1993, the very close lightning electromagnetic environment has been studied at the International Center for Lightning Research and Testing (ICLRT) at Camp Blanding, Florida. The electric field waveforms recorded in 1997 at six distances ranging from 10 to 500 m from the lightning channel, for a typical dart-leader/return-stroke sequence in triggered lightning, are shown as an example in Fig. 3. Note that the amplitude of the V-shaped waveform decreases and its duration increases with increasing distance from the lightning channel. With a few exceptions, the variation of amplitude as a function of distance is close to an inverse proportionality (Crawford et al. 2000 [17]), which is consistent with a more or less uniform distribution of leader charge along the bottom kilometer or so of the channel.

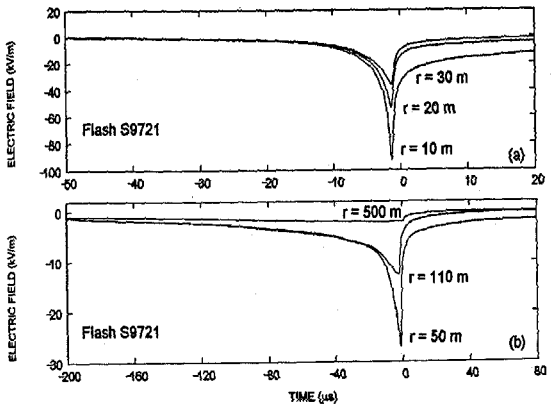

Fig. 3. Electric field waveforms of the first leader/return-stroke sequence of flash S9721 as recorded in 1997 at distances (a) 10, 20, and 30 m and (b) 50, 110, and 500 m at Camp Blanding, Florida. Adapted from Crawford et al. (1999) [18].

From 1993 through 1998, the rocket launching systems used at ICLRT had a height of typically 3 to 7 m (including the lightning strike rod) and were placed on the ground or on top of a wooden tower. Electric and magnetic fields produced by triggered lightning were measured after they had propagated over sandy soil. In order to minimize the influence of the triggering structure and of propagation effects due to the finite soil conductivity, in 1999 a new triggering facility was constructed at ICLRT. In this facility, the launcher was placed below ground level and was surrounded by a buried metallic grid having dimensions of 70 m by 70 m. The grid had a mesh size of 5 cm by 8 cm and was buried at a depth of up to 20 cm. The top of the underground launcher (about 4 m tall), which was nearly flush with the ground surface, was bonded via four symmetrically-arrayed metal straps to the buried grid. In order to increase the probability of lightning attachment to the instrumented launcher, a lightning strike rod was mounted on top of the launcher. The height of this rod above ground initially was 1 m and later was increased to 2 m.
Electric and magnetic fields and their rates of change (time derivatives) were measured in 1999 at distances of 15 and 30 m from the lightning strike rod. Electric field and electric field derivative data for a stroke that attached to the 1-m strike rod and exhibited a relatively straight and vertical channel are shown in Fig. 4. The E-field waveforms are displayed on a 100-μs time scale, while the dE/dt waveforms are displayed on a 10-μs time scale. This stroke transported negative charge to ground; its return-stroke current had a peak value of 15 kA. The E-fields in Fig. 4 exhibit the characteristic V-shaped waveforms discussed above. For the dE/dt waveforms, the zero crossing corresponds to the bottom of the V, so that the negative part of the dE/dt signature corresponds to the leader and the positive part to the return stroke. Note from Fig. 4 that at 15 m the dE/dt peak for the leader is a significant fraction of that for the return stroke. Uman et al. (2000) [19], who measured dE/dt at 10, 14 and 30 m at ICLRT in 1998 (the field propagation path was over sandy soil as opposed to propagation over a buried metallic grid), reported that for one event dE/dt for the dart leader at 14 m was more than 70 percent of the dE/dt for the corresponding return stroke.

3. Lightning Models:

3.1 General overview:

Any lightning model is an approximate mathematical construct designed to reproduce certain aspects of the physical processes involved in the lightning discharge. The basic assumptions of the model should be consistent with both the expected outputs of the model and the availability of quantities required as inputs to the model. No modeling is complete until model predictions are compared with experimental data; that is, model testing, often called validation, is a necessary component of any modeling. It is sometimes useful to distinguish between "predictive" and "engineering" models, although the distinction between the two types is not always clear. The former can be used for revealing additional, presently

unknown or poorly understood facets of the process being modeled. For example, the gas dynamic return-stroke models, discussed in Section 3.2, can be useful in gaining insights into the lightning energy balance and thunder generation mechanisms. These models are very difficult to test since many of outputs are not easy to observe. "Engineering" models, on the other hand, are primarily used as tools for the computation of certain, usually well understood quantities based on a few easy-to-obtain input parameters. Good examples are the engineering return-stroke models discussed in Section 3.5 that are primarily used, in conjunction with Maxwell's equations, for calculating the remote lightning electric and magnetic fields. These models are relatively easy to test using measured input parameters and measured electric and magnetic fields. We define four classes of lightning return stroke models. Most published models can be assigned to one, or sometimes two, of these four classes. The classes are primarily distinguished by the type of governing equations: (1) The first class of models is the gas dynamic models which are primarily concerned with the radial evolution of a short segment of the lightning channel and its associated shock wave. These models typically involve the solution of three gas dynamic equations (sometimes called hydrodynamic equations) representing the conservation of mass, of momentum, and of energy, coupled to two equations of state, with the input parameter being an assumed channel current versus time. Principal model outputs include temperature, pressure, and mass density as a function of radial coordinate and time. (2) The second class of models is the electromagnetic models that are usually based on a lossy antenna approximation to the lightning channel. These models involve a numerical solution of Maxwell's equations to find the current distribution along the channel from which the remote electric and magnetic fields can be computed.

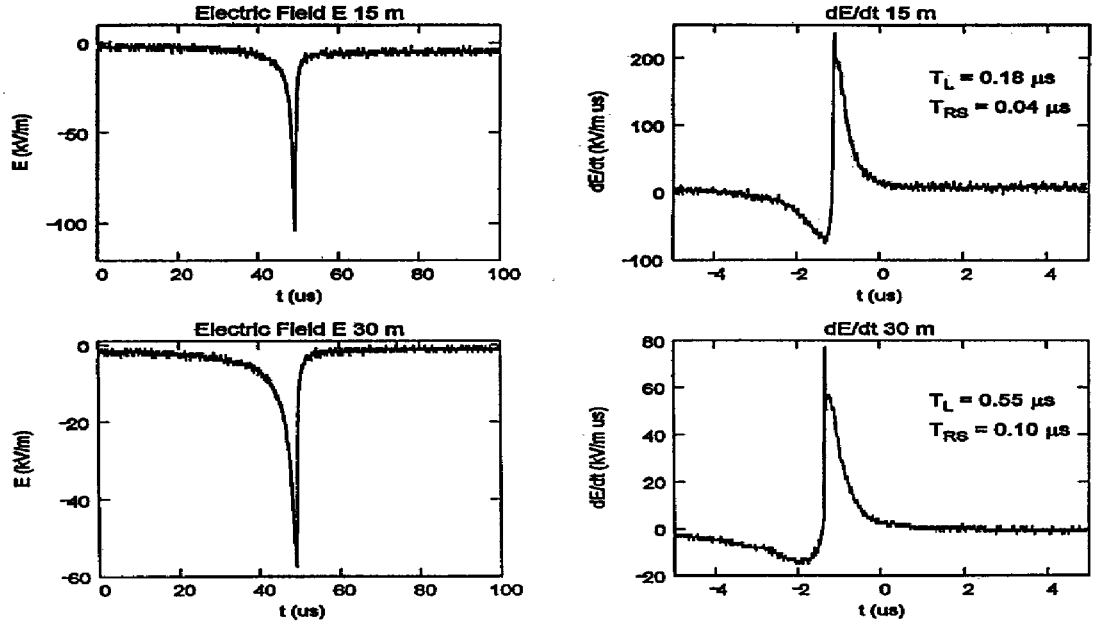

Fig. 4. Electric field and electric derivative (dE/dt) waveforms for stroke 2 in rocket-triggered flash S9918 measured at 15 and 30 m from the lightning channel at Camp Blanding, Florida. Adapted from Rakov et al. (2000) [20].

(3) The third class of models is the distributed-circuit models that can be viewed as an approximation to the electromagnetic models described above and that represent the lightning discharge as a transient process on a vertical transmission line characterized by resistance (R), inductance (L), and capacitance (C), all per unit length. (4) The fourth class of models is the engineering models in which a spatial and temporal distribution of the channel current (or the channel line charge density) is specified based on such observed lightning return-stroke characteristics as current at the channel base, the speed of the upward-propagating front, and the channel luminosity profile. In these models, the physics of the lightning return stroke is deliberately downplayed, and the emphasis is placed on achieving agreement between the model-predicted electromagnetic fields and those observed at distances from tens of meters to hundreds of kilometers. A characteristic feature of the engineering models is the small number of adjustable parameters, usually one or two besides the measured or assumed channel-base current.

Outputs of the electromagnetic, distributed-circuit, and engineering models can be directly used for the computation of electromagnetic fields, while the gas dynamic models can be used for finding R as a function of time, which is one of the parameters of the electromagnetic and distributed-circuit models. Since the distributed-circuit and engineering models generally do not consider lightning channel branches, they best describe subsequent strokes or first strokes before the first major branch has been reached by the return stroke, a time that is usually longer than the time required for the formation of the initial current peak at ground. If not otherwise specified, we assume that the lightning channel is straight and vertical and has no branches. The gas dynamic models are equally applicable to both first and subsequent strokes since they consider the radial evolution of a short segment of the channel. The electromagnetic models can be formulated for any channel geometry to represent either first or subsequent strokes. In the following, we will review each of the four classes of return-stroke models. Further discussion of lightning models is found in Rubinstein et al. (1995) [16], Thottappillil et al. (1997) [21], Rakov (1997) [22], Rakov and Uman (1998) [23], Gomes and Cooray (2000) [24], and in references given in these papers.

3.2 Gas dynamic models:

Gas dynamic models describe the behavior of a short segment of a cylindrical plasma column driven by the resistive heating caused by a specified time-varying current. Some models of this type were developed for laboratory spark discharges in air but have been used for or thought to be applicable to the lightning return stroke (e.g., Drabkina 1951 [25]; Braginskii 1958 [26]; Plooster 1970, 1971a, b [27-29]). Drabkina (1951) [25], assuming the spark channel pressure to be much greater than the ambient pressure, the so-called strong shock approximation, described the radial evolution of a spark channel and its associated shock wave as a function of the time-dependent energy injected into the channel. Braginskii (1958) [26] also used the strong-shock approximation to develop a spark channel model describing the time variation of such parameters as radius, temperature, and pressure as a function of the

input current. For a current I(t) linearly increasing with time t, he obtained the following expression for channel radius r(t) as presented by Plooster (1971b) [29]: r(t) . 9.35[I(t)]$^{1/3}$t$^{1/2}$ where r(t) is in centimeters, I(t) in amperes, and t in seconds. In the derivation of this expression, presumably applicable to the early stages of the discharge, Braginskii (1958) [26] set the electrical conductivity Φ of the channel at 2.22x10^{4} S m^{-1} and assumed the ambient air density to be 1.29 x 10^{-3} g cm^{-3}. For a known r(t), the resistance per unit channel length can be found as R(t) = [ΦBr^{2}(t)]$^{-1}$ and the energy input per unit length as

$$W(t) = \int_0^t I^2(\tau) R(\tau) d\tau$$

More recent gas-dynamic modeling algorithms, published by Hill (1971,1977a) [30,31], Plooster (1970, 1971a, b) [27-29], Strawe (1979) [32], Paxton et al. (1986, 1990) [33,34], Bizjaev et al. (1990) [35], and Dubovoy et al. (1991a, b, 1995) [36-38], can be briefly outlined as follows: It is assumed that (1) the plasma column is straight and cylindrically symmetrical, (2) the algebraic sum of positive and negative charges in any volume element is zero, and (3) local thermodynamic equilibrium exists at all times. Initial conditions, that are meant to characterize the channel created by the lightning leader, include temperature (of the order of 10,000E K), channel radius (of the order of 1 mm), and either pressure equal to ambient (1 atm) or mass density equal to ambient (of the order of 10^{-3} g cm^{-3}), the latter two conditions representing, respectively, the older and the newly-created channel sections. The initial condition assuming ambient pressure probably best represents the upper part of the leader channel since that part has had sufficient time to expand and attain equilibrium with the surrounding atmosphere, while the initial condition assuming ambient density is more suitable for the recently created, bottom part of the leader channel. In the latter case, variations in the initial channel radius and initial temperature are claimed to have little influence on model predictions (e.g., Plooster 1971b [29]; Dubovoy et al. 1995) [38]. The input current is assumed to rise to about 20 kA in some microseconds and then decay in some tens of microseconds. At each time step, (1) the electrical energy sources and (2) the radiation energy sources, and sometimes (3) the Lorentz force (Dubovoy et al. 1991a, b, 1995 [36-38]) are computed, and the gas dynamic equations are numerically solved for the thermodynamic and flow parameters of the plasma. The exact form of the gas dynamic equations and the set of variables for which the equations are solved differ from one study to another. Plooster (1970, 1971a, b) [27-29], for example, used five equations, including equations of conservation of mass, momentum, and energy, a definition for the radial gas velocity, and an equation of state for the gas, that were solved for the following five variables: radial coordinate, radial velocity, pressure, mass density, and internal energy per unit mass. As noted earlier, the gas dynamic models do not consider the longitudinal evolution of the lightning channel. They also usually ignore the electromagnetic skin effect (which Plooster (1971a) [28] found to be negligible), the corona sheath which presumably contains the bulk of the leader charge, and any heating of the air surrounding the current-carrying channel by preceding lightning processes. An attempt to include the previous heating in a gas dynamic model was made by Bizjaev et al. (1990) [35].

3.3 Electromagnetic models:

Electromagnetic return-stroke models based on the representation of the lightning channel as a lossy antenna have been proposed by Podgorski and Landt (1987) [39] and Moini et al. (1997) [40]. These models involve a numerical solution of Maxwell's equations using the method of moments (MOM) (e.g., Sadiku 1994 [41]), which yields the complete solution for channel current including both the antenna-mode current and the transmission-line-mode current (e.g., Paul 1994 [42]). The resistive loading used by Podgorski and Landt (1987) [39] was 0.7 Σ m^{-1} and that used by Moini et al. (1997) [40] was 0.065 Σ m^{-1}. In order to simulate the effect on the return-stroke velocity of the radially-formed corona surrounding the current-carrying channel core and presumably containing the bulk of the channel charge, Moini et al. (1997) [40] set the permittivity γ of the air surrounding the equivalent antenna to a value greater than γ_0 for the computation of the current distribution along the antenna. As a result, even without resistive loading, the phase velocity of an electromagnetic wave guided by the antenna $v_p = (:_0\gamma)^{-½}$ was reduced with respect to the velocity of light $c = (:_0\gamma_0)^{-½}$. The resistive loading further reduced v_p. The current distribution computed assuming the surrounding fictitious dielectric had permittivity γ and the antenna was resistively loaded was then allowed to radiate electromagnetic fields into free space characterized by $\gamma = \gamma_0$, $: = :_0$. The model of Moini et al. (1997) [40] considers a straight vertical channel and ignores any non-linear effects, while the model of Podgorski and Landt (1987) [39] deals with a three-dimensional channel of arbitrary shape and reportedly can include branches, strike object, upward connecting discharge, and non-linear effects during the attachment process. Podgorsky and Landt (1987) [39] do not give any model-predicted fields. Moini et al. (1997) [40] have demonstrated fairly good agreement between the model-predicted and typical measured electric fields at distances ranging from tens of meters to tens of kilometers. At 100 km, their model does not predict a field zero-crossing within 200 :s or so, and hence is inconsistent with typical measured fields at this distance (see Fig. 1).

3.4 Distributed-circuit models:

Distributed-circuit models consider the lightning channel to be an R-L-C transmission line for which voltage V and current I are solutions of the telegrapher's equations:

$$-\frac{\partial v(z',t)}{\partial z'} = L\frac{\partial I(z',t)}{\partial t} + RI(z',t) \qquad (1)$$

$$-\frac{\partial I(z',t)}{\partial z'} = C\frac{\partial v(z',t)}{\partial t} \qquad (2)$$

where R, L, and C are, respectively, the series resistance, series inductance, and shunt capacitance, all per unit length, zρ is the vertical coordinate specifying position on

the lightning channel, and t is the time. The equivalent transmission line is usually assumed to be charged (by the preceding leader) to a specified potential and then closed at the ground end with a specified earth resistance to initiate the return stroke. The second of the telegrapher's equations is equivalent to the continuity equation. Equations (1) and (2) can be derived from Maxwell's equations assuming that the electromagnetic waves propagating on (guided by) the line exhibit a quasi-transverse electromagnetic (quasi-TEM) field structure and that R, L, and C are constant (e.g., Agrawal et al. 1980 [43]). Note that the term "quasi-transverse electromagnetic field structure" implies that the transverse component of the total electric field is much greater than the z-directed component associated with a non-zero value of R (Paul 1994 [42]). The telegrapher's equations can be also derived using Kirchhoff's laws (e.g., Sadiku 1994 [41]) from the equivalent circuit shown in Fig. 5. In general,each of the transmission line parameters representing a return-stroke channel is a function of time and space; that is, the transmission line is nonlinear and non-

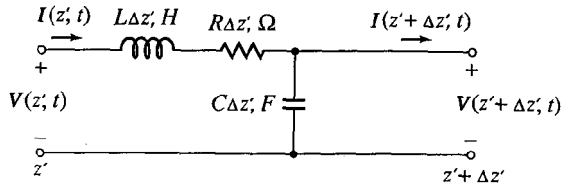

Fig. 5. The equivalent circuit for an elemental section of an R-L-C transmission line from which the telegrapher's equations (1) and (2) can be derived using Kirchhoff's laws in the limit as $\Delta z' \to 0$. In general, the transmission line parameters, R, L, and C, are each a function of z′ and t. The return path corresponds to the lightning channel image (assuming a perfectly conducting ground). All the information on the actual geometry of the transmission line is contained in L and C.

uniform (e.g., Rakov 1998 [44]). The channel inductance changes with time due to variation in the radius of the channel core that carries the z-directed channel current. The channel resistance changes with time due to variation in the electron density, heavy particle density, and the radius of the channel core. The channel capacitance changes with time mostly due to the neutralization of the radially-formed corona sheath that surrounds the channel core and presumably contains the bulk of the channel charge deposited by the preceding leader. For the case of a nonlinear transmission line, equations (1) and (2) are still valid if L and C are understood to be the dynamic (as opposed to the static) inductance and capacitance, respectively (e.g., Gorin 1985 [45]): L = MN/MI, C = MΔ/MV where N is the magnetic flux linking the channel, and Δ is the channel charge, both per unit length. An exact closed form solution of the telegrapher's equations can be generally obtained only in the case of R, L, and C all being constant. There is at least one exception to this latter statement: a nonlinear distributed-circuit model described by Baum and Baker (1990) [46] and Baum (1990b) [47], in which C is a function of charge density to simulate the radial-corona sheath. The telegrapher's equations representing this model admit exact solutions but only if R = 0. Linear distributed-circuit models have been used, for instance, by Oetzel (1968) [48], Price and Pierce (1977) [49] (R . 0.06 Σ m^{-1}), Little (1978) [50] (R = 1 Σ m^{-1}), and Takagi and Takeuti (1983) [51] (R = 0.08 Σ m^{-1}). Rakov (1998) [44] found that the behavior of electromagnetic waves guided by a linear R-L-C transmission line representing the pre-return-stroke channel formed by a dart leader and having R = 3.5 Σ m^{-1} is consistent with the observed luminosity profiles for the return stroke (Jordan and Uman 1983 [52]). If the line nonlinearites are taken into account, the solution of the telegrapher's equations requires the use of a numerical technique, for instance, a finite-difference method (Quinn 1987 [53]). Attempts to take into account the lightning channel nonlinearities using various simplifying assumption have been made by Gorin and Markin (1975) [54], Gorin (1985) [45], Baum and Baker (1990) [46], Baum (1990b) [47], Mattos and Christopoulos (1988, 1990) [55,56], and Kostenko (1995) [57]. The results presented by Gorin and Markin (1975) [54] are shown, as an example, in Figs. 6 and 7. Even if R, L, and C were constant, the application of the R-L-C transmission line model to

lightning is an approximation. Indeed, for a vertical lightning channel with the current equivalent return path being the vertical channel image (assuming a perfectly conducting ground) the validity of the TEM assumption is questionable, in particular near the return-stroke tip where a relatively large longitudinal component of electric field is present. Usually, a distributed-circuit model of the lightning return stroke is postulated without proper analysis of its applicability. Baum and Baker (1990) [46] represented the lightning channel "return path" by a cylinder coaxial with and enclosing the lightning channel. Clearly, the radius of the artificial outer return-path cylinder affects the L and C values of such a coaxial R-L-C transmission line model, although the dependence is rather weak. Note that the telegrapher's equations (1) and (2) are the same for any two-conductor transmission line (including a coaxial one), with all the information on the actual line geometry being contained in L and C.

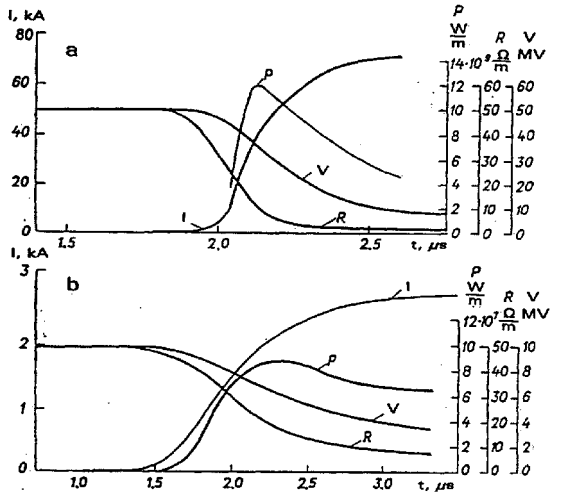

Fig. 6. Current, I voltage V, power per unit length P, and resistance per unit length R as a function of time t at a height of 300 m above ground as predicted by the distributed-circuit model of Gorin and Markin (1975) [54]. Profiles are given for (a) V_0 = 50 MV and an instantaneously discharged coronal sheath, and for (b) V_0 = 10 MV, and no corona sheath where V_0 is the initial uniform voltage on the channel due to charges deposited by the preceding leader. Adapted from Gorin and Markin (1975) [54].

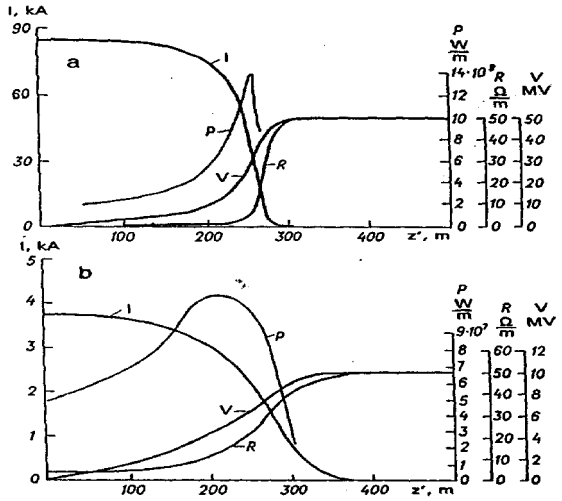

Fig. 7. Same as Fig. 6 but as a function of height zρ along the channel at a given instant time.

Strawe (1979) [32] proposed two versions of a distributed-circuit model that differ in the way that the value of R as a function of channel current and channel electrical conductivity was computed. In the first version, the conductivity was assumed to be constant so that R varied only because of channel expansion. In the second version, the conductivity was a function of channel temperature and pressure that were found using a model of the gas dynamic type. In both versions, L and C were assumed constant. An upward-going connecting discharge from earth of 100 m length was simulated as an R-L-C transmission line as well. The second version of Strawe's (1979) [32] model is actually a combination of a gas dynamic model and a distributed-circuit model. A combination of a gas dynamic model and a distributed-circuit model was also proposed by Baker (1990) [58], although the model was not described in detail. Electromagnetic fields calculated by Takagi and Takeuti (1983, Figs. 12 and 13) [51] and Price and Pierce (1977, Fig. 4) [49], who used linear distributed-circuit models, and by Mattos and Christopoulos (1990, Figs. 7-9) [55,56] and Baker (1990, Figs. 3 and 6) [58], who used nonlinear distributed-circuit models, are largely inconsistent with typical measured fields (see Fig. 1). Other authors do not present model-predicted electromagnetic fields.

3.5 Engineering models

An engineering return-stroke model, as defined here, is simply an equation relating the longitudinal channel current I (zρ,t) at any height zρ and any time t to the current I(0,t) at the channel origin, zρ = 0. An equivalent expression in terms of the line charge density Δ(zρ,t) on the channel can be obtained using the continuity equation (Thottappillil et al. 1997 [22]). Thottappillil et al. (1997) [21] distinguished between two components of the charge density at a given channel section, one component being associated with the return-stroke charge transferred through this channel

section and the other with the charge deposited at this channel section. As a result, their charge density formulation provides new insights into the physical mechanisms behind the models, generally not recognized in the longitudinal-current formulation.

3.5.1 Description of models

We first consider mathematical and graphical representations of some simple models and then categorize and discuss the most used engineering models based on their implications regarding the principal mechanism of the return-stroke process. Many engineering models can be expressed by the generalized current equation proposed by Rakov (1997) [22]:

$$I(z',t) = u(t - z'/v_f)P(z')I(0, t - z'/v) \qquad (3)$$

where u is the is the Heaviside function equal to unity for t ∃ zρ/v_f and zero otherwise, P(zρ) is the height-dependent current attenuation factor introduced by Rakov and Dulzon (1991) [59], v_f is the upward-propagating front speed (also called return-stroke speed), and v is the current-wave propagation speed. Table 2 summarizes P(zρ) and v for five engineering models, namely, the transmission line model TL (Uman and McLain 1969 [60]), not to be confused with the R-L-C transmission line models discussed above; the modified transmission line model with linear current decay with height, MTLL (Rakov and Dulzon 1987 [61]); the modified transmission line model with exponential current decay with heigh, MTLE (Nucci et al. 1988a [62]; the Bruce-Golde model, BG (Bruce and Golde 1941 [63]; and the travelling current source model, TCS (Heidler 1985 [64]. In Table 2, H is the total channel height, 8 is the current decay constant (assumed by Nucci et al. (1988a) [62] to be 2000 m) and c is the speed of light. If not specified otherwise, v_f is assumed to be constant. Front speeds decaying exponentially with time, which is equivalent to decaying linearly with height, as shown by Leise and Taylor (1977) [65], have also been used in an attempt to model the first stroke in a flash (e.g., Bruce and Golde 1941 [63]; Uman and McLain 1969 [60]; Dulzon and Rakov 1980 [66]). The three simplest models, TCS, BG, and TL, are illustrated in Fig. 8.

Table 2. P(zρ) and v in equation (3) for five engineering models.

Model	P(z′)	v
TL (Uman and McLain 1969)	1	v_f
MTLL (Rakov and Dulzon 1987)	1-z′/H	v_f
MTLE (Nucci et al. 1988a)	exp(-z′/λ)	v_f
BG (Bruce and Golde 1941)	1	∞
TCS (Heidler 1985)	1	-c

For all three models, we assume the same current waveform at the channel base ($z\rho$ = 0) and the same front speed represented in the $z\rho$- t coordinates by the slanted line labeled v_f. The current-wave speed is represented by the line labeled v which coincides with the vertical axis for the BG model and with the v_f line for the TL model. Shown for each model are current versus time waveforms at the channel base ($z\rho = 0$) and at heights $z\rho_1$ and $z\rho_2$. Because of the finite front propagation speed v_f, current at a height, say $z\rho_2$, begins with a delay $z\rho_2/v_f$ with respect to the current at the channel base. The dark portion of the waveform indicates current that actually flows through a given channel section, the blank portion being shown for illustrative purpose only. As seen in Fig. 8, the TCS, BG, and TL models are characterized by different current profiles along the channel, the difference being, from a mathematical point of view, due to the use of different values of v (listed in Table 2) in the generalized equation (3) with $P(z\rho) = 1$. It also follows from Fig. 8 that if the channel-base current were a step function, the TCS, BG, and TL models would be characterized by the same current profile along the channel, although established in an apparently different way in each of the three models. The most used engineering models can be grouped in two categories: the transmission-line-type models and the traveling-current-source-type models, summarized in Tables 3 and 4, respectively. Each model in Tables 3 and 4 is represented by both current and charge density equations. Table 3 includes the TL model and its two modifications: the MTLL and MTLE models. Rakov and Dulzon (1991) [59] additionally considered modified transmission line models with current attenuation factors other than the linear and exponential functions used in the MTLL and MTLE models, respectively. The transmission-line-type models can be viewed as incorporating a current source at the channel base which injects a specified current wave into the channel, that wave propagating upward (1) without either distortion or attenuation (TL), or (2) without distortion but with specified attenuation (MTLL and MTLE), as seen from the corresponding current equations given in Table 3. Table 4 includes the BG model (Bruce and Golde 1941 [63]), the TCS model (Heidler 1985 [64]), and the Diendorfer-Uman (DU) model (Diendorfer and Uman 1990 [67]). In the traveling-current-source-type models, the return-stroke current may be viewed as generated at the upward-moving return-stroke front and propagating downward. In the TCS model, current at a given channel section turns on instantaneously as this section is passed by the front, while in the DU model, current turns on gradually (exponentially with a time constant ϑ_D if $I(0,t+z\rho/c)$ were a step function). Channel current in the TCS model may be viewed as a downward-propagating wave originating at the upward-moving front. The DU model formulated in terms of current involves two terms (see Table 4), one being the same as the downward-propagating current in the TCS model that exhibits an inherent discontinuity at the upward-moving front (see Fig. 8), and the other one being an opposite polarity current which rises instantaneously to the value equal in magnitude to the current at the front and then decays exponentially with a time constant ϑ_D. The second current component in the DU model, which may be viewed merely as a "front modifier," propagates upward with the front and eliminates any current discontinuity at that front. The time

constant ϑ_D is the time during which the charge per unit length deposited at a given channel section by the preceding leader reduces to 1/*e* (about 37 percent) of its original value after this channel section is passed by the upward-moving front. Thottappillil and Uman (1993) [68] and Thottappillil et al. (1997) [21] assumed that ϑ_D = 0.1 :s. Diendorfer and Uman (1990) [67] considered two components of charge density, each released with its own time constant in order to match model predicted fields with measured fields. If ϑ_D = 0, the DU model reduces to the TCS model. In both

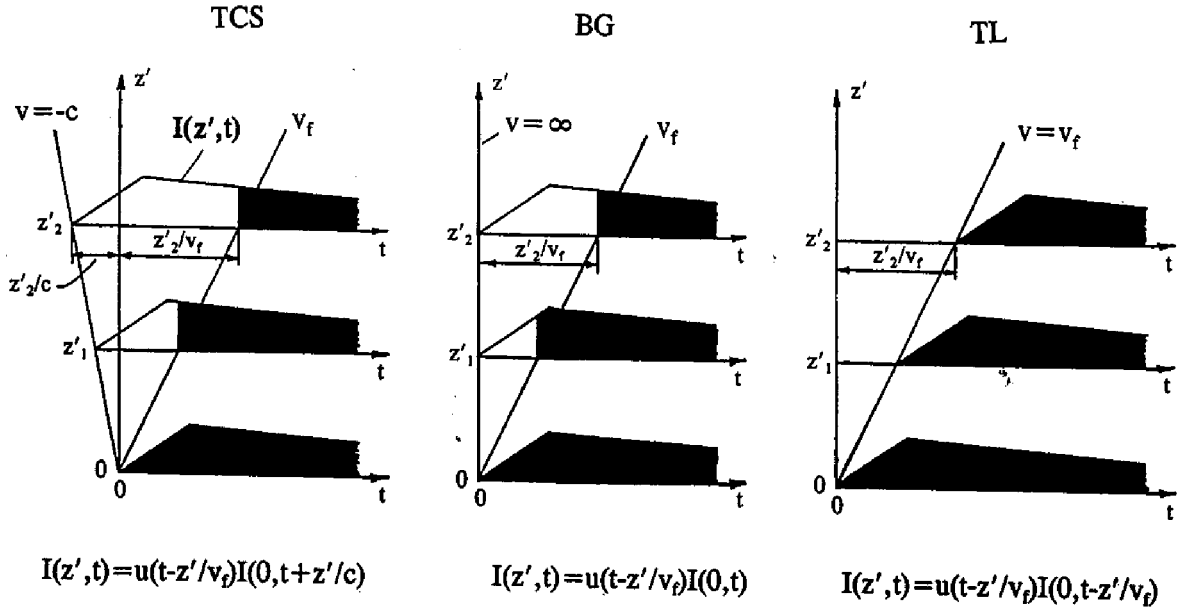

$$u(t-z'/v_f) = \begin{cases} 0 & t < z'/v_f \\ 1 & t \geq z'/v_f \end{cases}$$

v_f = front speed
v = current wave speed
c = speed of light

Fig. 8. Current versus time waveforms at ground ($z\rho$ = 0) and at two heights $z\rho_1$ and $z\rho_2$ above ground for the TCS, BG, and TL return-stroke models. Slanted lines labeled v_f represent upward speed of the return-stroke front, and lines labeled v represent speed of the return-stroke current wave. The dark portion of the waveform indicates current that actually flows through a given channel section. Note that the current waveform at $z\rho$ = 0 and v_f are the same for all three models. Adapted from Rakov (1997) [22].

Table 3. Transmission-line-type models for $t \geq z'/v_f$.

TL (Uman and McLain 1969)	$I(z',t) = I(0, t - z'/v)$ $\rho_L(z',t) = \dfrac{I(0, t - z'/v)}{v}$
MTLL (Rakov and Dulzon 1987)	$I(z',t) = \left(1 - \dfrac{z'}{H}\right) I(0, t - z'/v)$ $\rho_L(z',t) = \left(1 - \dfrac{z'}{H}\right) \dfrac{I(0, t - z'/v)}{v} + \dfrac{Q(z',t)}{H}$
MTLE (Nucci et al. 1988a)	$I(z',t) = e^{-z'/\lambda} I(0, t - z'/v)$ $\rho_L(z',t) = e^{-z'/\lambda} \dfrac{I(0, t - z'/v)}{v} + \dfrac{e^{-z'/\lambda}}{\lambda} Q(z',t)$

$Q(z',t) = \int_{z'/v}^{t} I(0, \tau - z/v) d\tau$ $\quad v = v_f = \text{const}$ $\quad H = \text{const}$ $\quad \lambda = \text{const}$

the TCS and DU models, current propagates downward at the speed of light. The TCS model reduces to the BG model if the downward current propagation speed is set equal to infinity instead of the speed of light. Although the BG model could be also viewed mathematically as a special case of the TL model with v replaced by infinity, we choose to include the BG model in the traveling-current-source-type model category. Thottappillil et al. (1991a) [69] mathematically generalized the DU model to include a variable upward front speed and a variable downward current wave speed, both separate arbitrary functions of height (this model was dubbed MDU where M stands for "modified"). A further generalization of the DU model (Thottappillil and Uman 1994) [70] involves a single height-variable time constant ϑ_D. Generalizations of the TCS model are discussed later in this section. The principal distinction between the two

Table 4. Traveling-current-source-type models for $t \geq z'/v_f$.

BG (Bruce and Golde 1941)	$I(z',t) = I(0,t)$ $\rho_L(z',t) = \dfrac{I(0, z'/v_f)}{v_f}$
TSC (Heidler 1985)	$I(z',t) = I(0, t + z'/c)$ $\rho_L(z',t) = -\dfrac{I(0, t + z'/c)}{c} + \dfrac{I(0, z'/v^*)}{v^*}$
DU (Diendorfer and Uman 1990)	$I(z',t) = I(0, t + z'/c) - e^{-(t - z'/v_f)/\tau_D} I(0, z'/v^*)$ $\rho_L(z',t) = -\dfrac{I(0, t + z'/c)}{c} - e^{-(t - z'/v_f)/\tau_D} \times$ $\times \left[\dfrac{I(0, z'/v^*)}{v_f} + \dfrac{\tau_D}{v^*} \dfrac{dI(0, z'/v^*)}{dt} \right] +$ $+ \dfrac{I(0, z'/v^*)}{v^*} + \dfrac{\tau_D}{v^*} \dfrac{dI(0, z'/v^*)}{dt}$

$v^* = v_f/(1+v_f/c)$ $\quad v_f = \text{const}$ $\quad \tau_D = \text{const}$

types of engineering models formulated in terms of current is the direction of the propagation of current wave: upward for the transmission-line-type models ($v = v_f$) and downward for the traveling-current-source-type models ($v = -c$). As noted earlier, the BG model can be viewed mathematically as a special case of either TCS or TL

model. The BG model includes a current wave propagating at an infinitely large speed and, as a result, the wave's direction of propagation is indeterminate. As in all other models, the BG model includes a front moving at a finite speed v_f. Note that, even though the direction of propagation of the current wave in a model can be either up or down, the direction of current is the same; that is, charge of the same sign is effectively transported to ground in both types of the engineering models. The TL model predicts (e.g., Uman et al. 1975 [71]) that, as long as (1) the height above ground of the upward-moving return-stroke front (as "seen" at the observation point) is much smaller than the distance r between the observation point on ground and the channel base, so that all contributing channel points are essentially equidistant from the observer, (2) the return-stroke front propagates at a constant speed, (3) the return-stroke front has not reached the top of the channel, and (4) the ground conductivity is high enough so that propagation effects are negligible, the vertical component E_z^{rad} of the electric radiation field (and the horizontal component of the magnetic radiation field) is proportional to the channel-base current I. The equation for electric radiation field E_z^{rad} is as follows,

$$E_z^{rad}(r,t) = -\frac{v}{2\pi\varepsilon_0 c^2 r} I(0, t - r/c) \qquad (4)$$

where γ_0 is the permittivity of free space, v is the upward propagation speed of the current wave, which is the same as the front speed v_f in the TL as well as in the MTLL and MTLE models, and c is the speed of light. For the most common return stroke lowering negative charge to ground, the sense of positive charge flow is upward so that current I, assumed to be upward-directed in deriving equation (4), by convention is positive, and E_z^{rad} by equation (4) is negative; that is, the electric field vector points in the negative z direction. Taking the derivative of this equation with respect to time, one obtains

$$\frac{\partial E_z^{rad}(r,t)}{\partial t} = -\frac{v}{2\pi\varepsilon_0 c^2 r} \frac{\partial I(0, t - r/c)}{\partial t} \qquad (5)$$

Equations (4) and (5) are commonly used, particularly the first one and its magnetic radiation field counterpart, found from $*B_N^{rad}* = *E_z^{rad}*/c$, for the estimation of the peak values of return-stroke current and its time derivative, subject to the assumptions listed prior to equation (4). Equations (4) and (5) have been used for the estimation of v from measured E_p/I_p and $(dE/dt)_p/(dI/dt)_p$, respectively, where the subscript "z" and superscript "rad" are dropped, and the subscript "p" refers to peak values. The expressions relating channel base current and electric radiation field far from the channel for the BG, TCS, and MTLE models are given by Nucci et al. (1990) [72]. General equations for computing electric and magnetic fields at ground are found, for example, in Rakov and Uman (1998) [23]. As stated in Section 3.1, a characteristic feature of the engineering models is the small number of adjustable parameters, usually one or two besides the channel-base current. In these models, the physics of the lightning return stroke is deliberately downplayed, and the emphasis is placed on achieving an agreement between model-predicted electromagnetic fields and those observed at distances from tens of meters to hundred of kilometers.

Heidler and Hopf (1994) [73] modified the TCS model to take into account wave reflections at ground and at the upward-moving front using the traveling-current-source current as an input to the model. The source current is the current associated with the upward-moving front, which can be viewed as derived from the charge density distribution deposited along the channel by the preceding leader (e.g., Thottappillil et al. 1997 [21]). Both upward and downward waves behind the upward-moving front propagate at the speed of light, and the resultant reflection coefficient at the front is a function of v_f and v = c. The channel-base current in this model depends on the reflection coefficient at the strike point and on the initial charge density distribution along the channel. Heidler and Hopf (1995) [74] further modified the TCS model expressing the source current, and therefore the initial charge density distribution along the channel, in terms of the channel-base current and current reflection coefficient at ground. Cvetic and Stanic (1997) [75] proposed a model from which the TCS and DU models can be derived as special cases. Within the concept of the TCS model, they specify independently the channel-base current and the initial charge density distribution along the channel. The resultant current distribution along the channel is determined using the equation of current continuity.

3.5.2 Testing model validity

Two primary approaches to the testing of engineering models have been used: The first approach involves using a *typical* channel-base current waveform and a *typical* return-stroke propagation speed as model inputs and then comparing the model-predicted electromagnetic fields with *typical* observed fields. The second approach involves using the channel-base current waveform and the propagation speed measured for the same *individual* event and comparing computed fields with measured fields for that same *specific* event. The second approach is able to provide a more definitive answer regarding model validity, but it is feasible only in the case of triggered-lightning return strokes or natural lightning strikes to tall towers where channel-base current can be measured. In the field calculations, the channel is generally assumed to be straight and vertical with its origin at ground ($z\rho = 0$), conditions which are expected to be valid for subsequent strokes, but potentially not for first strokes. The channel length is usually not specified unless it is an inherent feature of the model, as is the case for the MTLL model (e.g., Rakov and Dulzon 1987 [61]). As a result, the model-predicted fields may not be meaningful after 25-75 :s, the expected time it takes for the return-stroke front to traverse the distance from ground to the cloud charge source.

"*Typical-return-stroke*" *approach*. This approach has been adopted by Nucci et al. (1990) [72], Rakov and Dulzon (1991) [59], and Thottappillil et al. (1997) [21]. Nucci et al. (1990) [72] identified four characteristic features in the fields at 1 to 200 km measured by Lin et al. (1979) [2] (see Fig. 1) and used those features as a benchmark for their validation of the TL, MTLE, BG, and TCS models. The characteristic features include (1) a sharp initial peak that varies approximately as the inverse distance beyond a kilometer or so in both electric and magnetic fields, (2) a

slow ramp following the initial peak and lasting in excess of 100 :s for electric fields measured within a few tens of kilometers, (3) a hump following the initial peak in magnetic fields within a few tens of kilometers, the maximum of which occurs between 10 and 40 :s, and (4) a zero crossing within tens of microseconds of the initial peak in both electric and magnetic fields at 50 to 200 km. For the current (see Fig. 9) and other model characteristics assumed by Nucci et al. (1990) [72], feature (1) is reproduced by all the models examined, feature (2) by all the models except for the TL model, feature (3) by the BG, TL and TCS models, but not by the MTLE model, and feature (4) only by the MTLE model, but not by the BG, TL, and TCS models, as illustrated in Figs. 10 and 11.

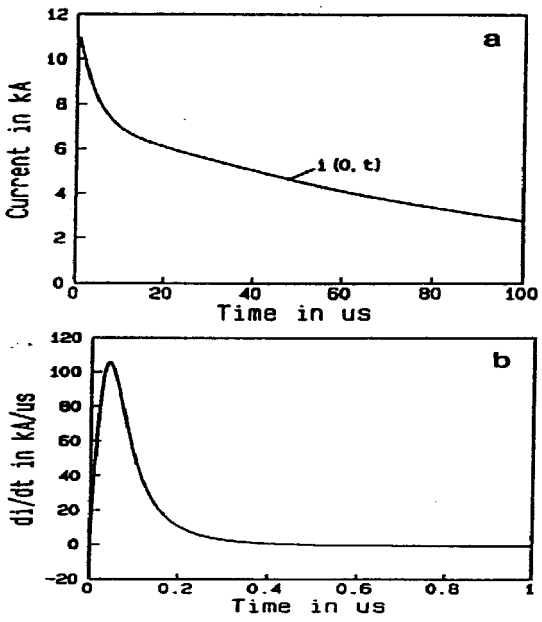

Fig. 9. (a) Current at ground level and (b) current derivative used by Nucci et al. (1990) [72], Rakov and Dulzon (1991) [59], and Thottappillil et al. (1997) [21] for the validity of return-stroke models by the "typical-return-stroke" approach. Adapted from Nucci et al. (1990) [72].

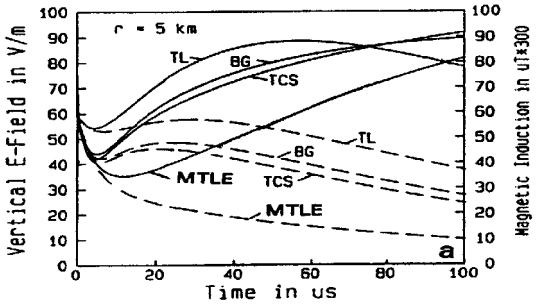

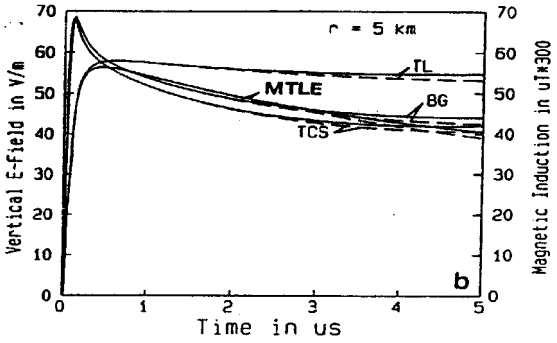

Fig. 10. Calculated electric (left scaling, solid lines) and magnetic (right scaling, dashed lines) fields for four models at a distance r = 5 km for (a) 100 :s and (b) the first 5 :s. Adapted from Nucci et al. (1990) [72].

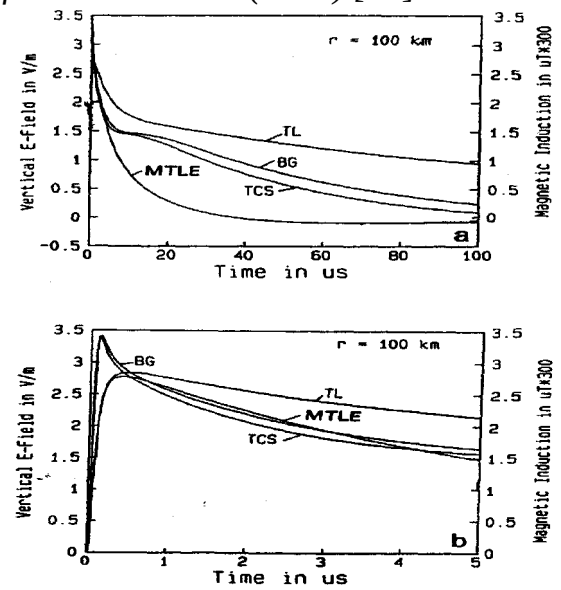

Fig. 11. Calculated electric (left scaling) and magnetic (right scaling) fields for four models at a distance r = 100 km for (a) 100 :s and (b) the first 5 :s. Adapted from Nucci et al. (1990) [72].

Diendorfer and Uman (1990) [67] showed that the DU model reproduces features (1), (2), and (3), and Thottappillil et al. (1991b) [76] demonstrated that a relatively insignificant change in the channel-base current waveform (well within the range of typical waveforms) allows the reproduction of feature (4), the zero crossing, by the TCS and DU models. Rakov and Dulzon (1991) [59] showed that the MTLL model reproduces features (1), (2), and (4). The observed sensitivity of the distant field waveforms predicted by the TCS and DU models to the variations in the channel-base current waveform has important implications for the testing of models. Indeed, since appreciable variation in the current waveform is a well documented fact (e.g., Uman 1987 [77], Table 7.2), the relatively narrow range of observed zero-crossing times (e.g., Uman (1987 [77], Table 7.1) appears inconsistent with the TCS and DU models. On the other hand, the experimental field data (Fig. 1) might be biased toward earlier zero-crossing times and more pronounced opposite polarity overshoots due to the following two reasons. First, the oscilloscope sweep of 200 :s was

insufficient to measure relatively long zero crossing times. Second, the initial rising portion of the waveform was apparently not always completely recorded (the first recorded point on the waveform was 2.5 :s prior to the time of trigger) and, as a result, the zero field level apparently was sometimes set at a point on the waveform that was higher than the actual zero field level. Nucci et al. (1990) [72] conclude from their study that all the models evaluated by them using measured fields at distances ranging from 1 to 200 km predict reasonable fields for the first 5-10 :s, and all models, except the TL model, do so for the first 100 :s.

Thottappillil et al. (1997) [21] noted that measured electric fields at tens to hundreds of meters from triggered lightning (e.g., Uman et al. 1994 [78]; Rakov et al. 1998 [79]) exhibit a characteristic flattening within 15 :s or so, as seen in Fig. 3. Electric fields predicted at 50 m by the BG, TL, MTLL, TCS, MTLE, and DU models are shown in Fig. 12 taken from Thottappillil et al. (1997) [21]. As follows from this Figure, the BG, MTLL, TCS, and DU models, but not the TL and MTLE models, are consistent with measured fields presented in Fig. 3.

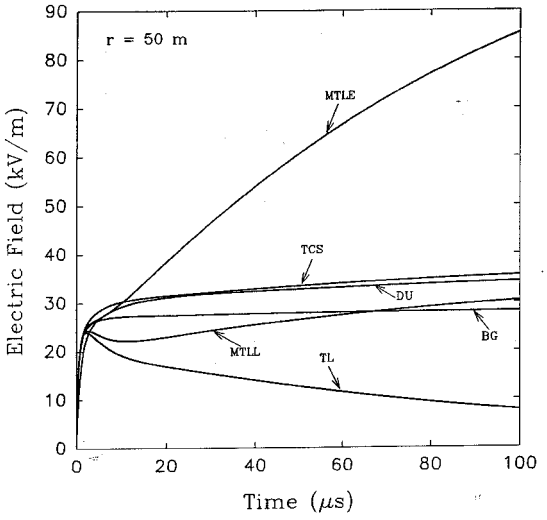

Fig. 12. Calculated electric fields for six return-stroke models at a distance r = 50 m, to be compared with typical measured return-stroke field at 50 m presented in Fig. 3. Note that only the upward-going portion of the waveforms shown in Fig. 3 is due to the return stroke, the downward-going portion being due to the preceding dart leader. Adapted from Thottappillil et al. (1997) [21].

"*Specific-return-stroke*" *approach*. This approach has been adopted by Thottappillil and Uman (1993) [68] who compared the TL, TCS, MTLE, DU, and MDU models. They used 18 sets of three simultaneously-measured features of triggered-lightning return strokes: channel-base current, return-stroke propagation speed, and electric field at about 5 km from the channel base, the data previously used by Willett et al. (1989) [80] for their analysis of the TL model. It has been found that the TL, MTLE, and DU models each predict the measured initial electric field peaks within an error whose mean absolute value is about 20 percent, while the TCS model has a mean absolute error about 40 percent.

4. Summary:

The overall results of testing the validity of the engineering return-stroke models can be summarized as follows: (a) The relation between the initial field peak and the initial current peak is reasonably well predicted by the TL, MTLL, MTLE, and DU models, (b) Electric fields at tens of meters from the channel after the first 10-15 :s are reasonably reproduced by the MTLL, BG, TCS and DU model, but not by the TL and MTLE models, and (c) From the standpoint of the overall field waveforms at 5 km (the only distance at which the "specific-return-stroke" model validation approach has been used) all the models should be considered less than adequate. Based on the entirety of the testing results and mathematical simplicity, we rank the engineering models in the following descending order: MTLL, DU, MTLE, TSC, BG, and TL. However, the TL model is recommended for the estimation of the initial field peak from the current peak or conversely the current peak from the field peak, since it is the mathematically simplest model with a predicted peak field/peak current relation that is equally or more accurate than that of the more mathematically complex engineering models.

References:

[1] V.A. Rakov, "Lightning electric and magnetic fields," in *Proc. 13th Int. Zurich Symp. on Electromagnetic Compatibility*, Zurich, Switzerland, 1999, pp. 561-566.

[2] Y.T. Lin, M.A. Uman, J.A. Tiller, R.D. Brantley, W.H. Beasley, E.P. Krider, and C.D. Weidman, "Character-ization of lightning return stroke electric and magnetic fields from simultaneous two-station measurements," *J. Geophys. Res.*, vol. 84, pp. 6307-6314, 1979.

[3] Y.T. Lin, M.A. Uman, and R.B. Standler, "Lightning return stroke models," *J. Geophys. Res.*, vol. 85, pp. 1571-1583, 1980.

[4] E.P. Krider and C. Guo, "The peak electromagnetic power radiated by lightning return strokes," *J. Geophys. Res.*, vol. 88, pp. 8471-8474, 1983.

[5] R. Thottappillil, V.A. Rakov, M.A. Uman, W.H. Beasley, M.J. Master, and D.V. Shelukhin, "Lightning subsequent stroke electric field peak greater than the first stroke peak and multiple ground terminations," *J. Geophys. Res.*, vol. 97, pp. 7503-7509, 1992.

[6] V.A. Rakov, M.A. Uman, and R. Thottappillil, "Review of Lighting Properties from Electric Field and TV Observations," *J. Geophys. Res.*, vol. 99, 10745-10750, 1994.

[7] M.J. Master, M.A. Uman, W.H. Beasley, and M. Darveniza, "Lightning induced voltages on power lines: Experiment," *IEEE Trans. Power. App. Syst.*, vol. 103, pp. 2519-2529, 1984.

[8] V. Cooray, and S. Lundquist, "On the character-istics of some radiation fields from lightning and their possible origin in positive ground flashes," *J. Geophys. Res.*, vol. 87, pp. 11,203-214, 1982.

[9] C.D. Weidman and E.P. Krider, "The fine structure of lightning return stroke wave forms," *J. Geophys. Res.*, vol. 83, pp. 6239-6247, 1978.

[10] C.D. Weidman and E.P. Krider, "Submicrosecond risetimes in lightning return-stroke fields," *Geophys. Res*. Lett., vol. 7, pp. 955-958, 1980a.
[11] C.D. Weidman and E.P. Krider, "Variations a L'Echelle submicroseconde des champs electromagnetiques rayonnes par la foudre," *Ann. Telecommun*., vol. 39, pp. 165-174, 1984.
[12] C.D. Weidman, "The submicrosecond structure of lightning radiation fields, *Ph.D. Dissertation*, Univ. Arizona, Tucson, 1982.
[13] M.A. Uman, C.E. Swanberg, J.A. Tiller, Y.T. Lin, and E.P. Krider, E.P., "Effects of 200 km propagation in Florida, lightning return stroke electric fields," *Radio Sci.*, vol. 11, pp. 985-990, 1976.
[14] V. Cooray and S. Lundquist, "Effects of propagation on the rise times and the initial peaks of radiation fields from return strokes," *Radio Sci.*, vol. 18, pp. 409-15, 1983.
[15] E.M. Thomson, P. Medelius, M. Rubinstein, M.A. Uman, J. Johnson, and J.W. Stone, "Horizontal electric fields from lightning return strokes," *J. Geophys. Res*., vol. 93, pp. 2429-2441, 1988.
[16] M. Rubinstein, F. Rachidi, M.A. Uman, R. Thottappillil, V.A. Rakov, and C.A. Nucci, "Characterization of vertical electric fields 500 m and 30 m from triggered lightning," *J. Geophys. Res.*, vol. 100, pp. 8863-8872, 1995.
[17] D.E. Crawford, V.A. Rakov, M.A. Uman, G.H. Schnetzer, K.J. Rambo, and M.V. Stapleton, "The close lightning electromagnetic environment: Leader electric field change vs. distance," J. Geophys. Res., submitted, 2000.
[18] D.E. Crawford, V.A. Rakov, M.A. Uman, G.H. Schnetzer, K.J. Rambo, and M.V. Stapleton, "Multiple-station measurements of triggered-lightning electric and magnetic fields," in *Proc. 11th Int. Conf. on Atmospheric Electricity*, Guntersville, Alabama, pp. 154-157, 1999.
[19] M. A. Uman, V.A. Rakov, G.H. Schnetzer, K.J. Rambo, D.E. Crawford, and R.J. Fisher, "Time derivative of the electric field 10, 14, and 30 m from triggered lightning strokes," *J. Geophys. Res*., vol. 105, pp. 15,557-595, 2000.
[20] V.A. Rakov, M.A. Uman, D. Wang, K.J. Rambo, D.E. Crawford, and G.H.Schnetzer, "Lightning properties from triggered-lightning experiments at Camp Blanding, Florida (1997-1999)," in *Proc. of the 25th Int. Conf. on Lightning Protection*, Rhodes, Greece, September 18-22, 2000, pp. 54-59.
[21] R. Thottappillil, R.A. Rakov, and M.A. Uman, "Distribution of charge along the lightning channel: Relation to remote electric and magnetic fields and to return stroke models," *J. Geophys. Res*., vol. 102, pp. 6887-7006, 1997.
[22] V.A. Rakov, "Lightning electromagnetic fields: Modeling and measurements," in *Proc. 12th Int. Zurich Symp. on Electromagnetic Compatibility*, Zurich, Switzerland, 1997, pp. 59-64.
[23] V.A. Rakov and M.A. Uman, "Review and evaluation of lightning return stroke models including some aspects of their application," *IEEE Trans. on Electromagn. Compat*., vol. 40, pp. 403-426, 1998.
[24] C. Gomes and V. Cooray, "Concepts of lightning return stroke models," *IEEE Trans. on Electromagnetic Compatibility*, vol. 42, pp. 82-96.

[25] S.I. Drabkina, "The theory of the development of the spark channel," *J. Exper. Theoret. Phys*., (English translation, AERE LIB/Trans. 621, Harwell, Berkshire, England.), vol. 21, pp. 473-83, 1951.

[26] S.I. Braginskii, "Theory of the development of spark channel," *Sov. Phys. JETP*, vol. 34, pp. 1068-1074, 1958.

[27] M.N. Plooster, "Shock waves from line sources: Numerical solutions and experimental measurements," *Phys. Fluids*, vol. 13, pp. 2665-2675, 1970.

[28] M.N. Plooster, "Numerical simulation of spark discharges in air," Phys. Fluids, vol. 14, pp. 2111-2123, 1971a.

[29] M.N. Plooster, "Numerical model of the return stroke of the lightning discharge," *Phys. Fluids*, vol. 14, pp. 2124-2133, 1971b.

[30] R.D. Hill, "Channel heating in return stroke lightning," *J. Geophys. Res*., vol. 76, pp. 637-645, 1971.

[31] R.D. Hill, "Energy dissipation in lightning," *J. Geophys. Res*., vol. 82, pp. 4967-4968, 1977a.

[32] D.F. Strawe, "Non-linear modeling of lightning return strokes," in *Proc. of the Federal Aviation Administration/Florida Institute of Technology Workshop on Grounding and Lightning Technology*, Melbourne, Florida, Report FAA-RD-79-6, pp. 9-15, 1979.

[33] A.H. Paxton, R.L. Gardner, and L. Baker, "Lightning return stroke: A numerical calculation of the optical radiation," *Phys. Fluids*, vol. 29, pp. 2736-2741, 1986.

[34] A.H. Paxton, R.L. Gardner, and L. Baker, "Lightning return stroke: A numerical calculation of the optical radiation," in *Lightning Electromagnetics*, , New York: Hemisphere, 1990, pp. 47-61.

[35] A.S. Bizjaev, V.P. Larionov, and E.H. Prokhorov, "Energetic characteristics of lightning channel," in *Proc. 20th Int. Conf. on Lightning Protection*, Interlaken, Switzerland, pp. 1.1/1-3, 1990.

[36] E.I. Dubovoy, V.I. Pryazhinsky, and G.I. Chitanava, "Calculation of energy dissipation in lightning channel," *Meteorologiya i Gidrologiya*, vol. 2, pp. 40-45, 1991a.

[37] E.I. Dubovoy, V.I. Pryazhinsky, and V.E. Bondarenko, "Numerical modeling of the gasodynamical parameters of a lightning channel and radio-sounding reflection," *Izvestiya AN SSSR-Fizika Atmosfery i Okeana* , vol. 27, pp. 194-203, 1991b.

[38] E.I. Dubovoy, M.S. Mikhailov, A.L. Ogonkov, and V.I. Pryazhinsky, "Measurement and numerical modeling of radio sounding reflection from a lightning channel," *J. Geophys. Res*., vol. 100, pp. 1497-502, 1995.

[39] A.S. Podgorski, and J.A. Landt, "Three dimensional time domain modelling of lightning," *IEEE Trans. Power Del*., vol. 2, pp. 931-938, 1987.

[40]] R. Moini, V.A. Rakov, M.A. Uman, and B. Kordi, "An antenna theory model for the lightning return stroke," in *Proc. 12th Int. Zurich Symp. on Electromagnetic Compatibility*, Zurich, Switzerland, 1997, pp. 149-152.

[41] M.N.O. Sadiku, *Elements of Electromagnetics*, Orlando, Florida: Sounders College, p. 821, 1994.

[42] C.R. Paul, "Analaysis of milticonductor transmission lines," New York: Wiley-Interscience, 1994.
[43] A.K. Agrawal, H.J. Price, and S.H. Gurbaxani, S.H. "Transient response of multiconductor transmission lines excited by a non-uniform electromagnetic field," *IEEE Trans. on Electromagnetic Compatibility*, May 1980, vol. EMC-22, pp. 119-129.
[44] V.A. Rakov, "Some inferences on the propagation mechanisms of dart leaders and return strokes," *J. Geophys. Res*., vol. 103, pp. 1879-1887, 1998.
[45] B.N. Gorin, "Mathematical modeling of the lightning return stroke," *Elektrichestvo*, vol. 4, pp. 10-16, 1985.
[46] C.E. Baum and L. Baker, "Analytic return-stroke transmission-line model," in *Lightning Electromagnetics*, ed. R.L. Gardner, New York: Hemisphere, 1990, pp. 17-40.
[47] C.E. Baum, "Return-stroke initiation," in *Lightning Electromagnetics*, ed. R.L. Gardner, New York: Hemisphere, 1990b, pp. 101-114.
[48] G.N. Oetzel, "Computation of the diameter of a lightning return stroke," *J. Geophys. Res.*, vol. 73, pp. 1889-1896, 1968.
[49] G.H. Price and E.T. Pierce, "The modeling of channel current in the lightning return stroke," *Radio Sci.*, vol. 12, pp. 381-388, 1977.
[50] P.F. Little, "Transmission line representation of a lightning return stroke," *J. Phys. D: Appl. Phys.*, vol. 11, pp. 1893-1910, 1978.
[51] N. Takagi and T. Takeuti, T. 1983. Oscillating bipolar electric field changes due to close lightning return strokes," *Radio Sci*., vol. 18, pp. 391-398, 1983.
[52] D.M. Jordan and M.A. Uman, "Variation in light intensity with height and time from subsequent lightning return strokes," *J. Geophys. Res.*, vol. 88, pp. 6555-6562, 1983.
[53] D.W. Quinn, "Modeling of lightning," *Mathematics and Computer Simulation*, vol. 29, pp. 107-118, 1987.
[54] B.N. Gorin and V.I. Markin, "Lightning return stroke as a transient process in a distributed system," *Trudy ENIN*, 1975, vol. 43, pp. 114-130.
[55] M.A. da F. Mattos and C. Christopoulos, "A nonlinear transmission line model of the lightning return stroke," *IEEE Trans. Electromagn. Compat.*, vol. 30, pp. 401-406, 1988.
[56] M.A. da F. Mattos, and C. Christopoulos, "A model of the lightning channel, including corona, and prediction of the generated electromagnetic fields," *J. Phys. D: Appl. Phys.*, vol. 23, pp. 40-6, 1990.
[57] M.V. Kostenko, "Electrodynamic characteristics of lightning and their influence on disturbances of high-voltage lines," *J. Geophys. Res.*, vol. 100, pp. 2739-2747, 1995.
[58] L. Baker, "Return-stroke transmission line model," in *Lightning Electromagnetics*, ed. R.L. Gardner, New York: Hemisphere, 1990, pp. 63-74.
[59] V.A. Rakov and A.A. Dulzon, "A modified transmission line model for lightning return stroke field calculations," in *Proc. 9th Int. Zurich. Symp. on Electromagnetic Compatibility*, Zurich, Switzerland, 1991, pp. 229-235.

[60] M.A. Uman and D.K. McLain, "Magnetic field of the lightning return stroke," *J. Geophys. Res.*, vol. 74, pp. 6899-6910, 1969.

[61] V.A. Rakov and A.A. Dulzon, "Calculated electromagnetic fields of lightning return stroke," *Tekh. Elektrodinam*., vol. 1, pp. 87-89, 1987.

[62] C.A. Nucci, C. Mazzetti, F. Rachidi, and M. Ianoz, "On lightning return stroke models for LEMP calculations," in *Proc. 19th Int. Conf. on Lightning Protection*, Graz, Austria, 1988a, pp. 463-469.

[63] C.E.R. Bruce and R.H. Golde, "The lightning discharge," *J. Inst. Elec. Eng*., vol. 88, pp. 487-520, 1941.

[64] F. Heidler, "Traveling current source model for LEMP calculation," in *Proc. 6th Int. Zurich Symp. on Electromagnetic Compatibility*, Zurich, Switzerland, 1985, pp. 157-162.

[65] J.A. Leise and W.L. Taylor, "A transmission line model with general velocities for lightning," *J. Geophys. Res.*, vol. 82, pp. 391-396, 1977.

[66] A.A. Dulzon and V.A. Rakov, "Estimation of errors in lightning peak current measurements by frame aerials," *Izvestiya VUZov SSSR-Energetika*, vol. 11, pp. 101-4, 1980.

[67] G. Diendorfer and M.A. Uman, "An improved return stroke model with specified channel-base current," *J. Geophys. Res.*, vol. 95, pp. 13,621-44, 1990.

[68] R. Thottappillil and M.A. Uman, "Comparison of lightning return-stroke models," *J. Geophys. Res.*, vol. 98, pp. 22,903-914, 1993.

[69] R. Thottappillil, D.K. McLain, M.A. Uman, and G. Diendorfer, "Extention of the Diendorfer-Uman lightning return stroke model to the case of a variable upward return stroke speed and a variable downward discharge current speed," *J. Geophys. Res.*, vol. 96, pp. 17,143-150, 1991a.

[70] R. Thottappillil and M.A. Uman, "Lightning return-stroke model with height-variable discharge time constant," *J. Geophys. Res.*, vol. 99, pp. 22,773-780, 1994.

[71] M.A. Uman, D.K. McLain, and E.P. Krider, "The electromagnetic radiation from a finite antenna," *Am. J. Phys*., vol. 43, pp. 33-38, 1975.

[72] C.A. Nucci, G. Diendorfer, M.A. Uman, F. Rachidi, M. Ianoz, and C. Mazzetti, "Lightning return stroke current models with specified channel-base current: a review and comparison. *J. Geophys. Res.*, vol. 95, pp. 20,395-408, 1990.

[73] F. Heidler and C. Hopf, "Lightning current and lightning electromagnetic impulse considering current reflection at the Earth's surface," in *Proc. 22nd Int. Conf. on Lightning Protection*, Budapest, Hungary, 1994, Paper R 4-05.

[74] F. Heidler and C. Hopf, "Influence of channel-base current and current reflections on the initial and subsidiary lightning electromagnetic field peak," *in Proc. 1995 Int. Aerospace and Ground Conf. on Lightning and Static Electricity*, Williamsburg, Virginia, USA, 1995, pp. 18/1-18/10.

[75] J.M. Cvetic and B.V. Stanic, "LEMP calculation using an improved return stroke model," in *Proc. 12th Int. Zurich Symp. On Electromagnetic Compatibility*, Zurich, Switzerland, pp. 77-82, 1997.

[76] R. Thottappillil, M. A. Uman, and G. Diendorfer, "Influence of channel base current and varying return stroke speed on the calculated fields of three important

return stroke models," *in Proc. 1991 Int. Conf. on Lightning and Static Electricity*, Cocoa Beach, Florida, 1991b, pp. 118.1-118.9.

[77] M. A. Uman, *The Lightning Discharge*, San Diego: Academic Press, 377 p., 1987.

[78] M.A. Uman, V.A. Rakov, V. Versaggi, R. Thottappillil, A. Eybert-Berard, L. Barret, J.-P. Berlandis, B. Bador, P.P. Barker, S.P. Hnat, J.P. Oravsky, T.A. Short, C.A. Warren, and R. Bernstein, "Electric fields close to triggered lightning," in *Proc. EMC'94 ROMA, Int. Symposium on Electromagnetic Compatibility*, Rome, Italy, 1994, pp. 33-37.

[79] V.A. Rakov, M.A. Uman, K.J. Rambo, M.I. Fernandez, R.J. Fisher, G.H. Schnetzer, R. Thottappillil, A. Eybert-Berard, J.P. Berlandis, P. Lalande, A. Bonamy, P. Laroche, and A. Bondiou-Clergerie, "New insights into lightning processes gained from triggered-lightning experiments in Florida and Alabama," *J. Geophys. Res.*, vol. 102, pp. 14, 117-130, 1998.

[80] J.C. Willett, Bailey, V.P. Idone, A. Eybert-Berard, and L. Barret, "Submicrosecond intercomparison of radiation fields and currents in triggered lightning return strokes based on the transmission-line model," *J. Geophys. Res.*, vol. 94, pp. 13,275-286, 1989.

Finished